

Accepted Manuscript

Silicate-based bioceramic scaffolds for dual-lineage regeneration of osteochondral defect

Varitsara Bunpetch, Xiaoran Zhang, Tian Li, Junxin Lin, Ewetse Paul Maswikiti, Yan Wu, Dandan Cai, Jun Li, Shufang Zhang, Chengtie Wu, Hongwei Ouyang



PII: S0142-9612(18)30802-0

DOI: <https://doi.org/10.1016/j.biomaterials.2018.11.025>

Reference: JBMT 18989

To appear in: *Biomaterials*

Received Date: 9 August 2018

Revised Date: 12 November 2018

Accepted Date: 14 November 2018

Please cite this article as: Bunpetch V, Zhang X, Li T, Lin J, Maswikiti EP, Wu Y, Cai D, Li J, Zhang S, Wu C, Ouyang H, Silicate-based bioceramic scaffolds for dual-lineage regeneration of osteochondral defect, *Biomaterials* (2018), doi: <https://doi.org/10.1016/j.biomaterials.2018.11.025>.

This is a PDF file of an unedited manuscript that has been accepted for publication. As a service to our customers we are providing this early version of the manuscript. The manuscript will undergo copyediting, typesetting, and review of the resulting proof before it is published in its final form. Please note that during the production process errors may be discovered which could affect the content, and all legal disclaimers that apply to the journal pertain.

Silicate-based bioceramic scaffolds for dual-lineage regeneration of osteochondral defect

Varitsara Bunpetch^{1,2}, Xiaoan Zhang^{1,2}, Tian Li⁵, Junxin Lin^{1,2}, Ewetse Paul Maswikiti^{1,2}, Yan Wu⁸, Dandan Cai^{1,2}, Jun Li^{1,2}, Shufang Zhang^{1,2,7}, Chengtie Wu^{*5,7} Hongwei Ouyang^{*1,2,3,4,6,7}

¹Dr. Li Dak Sum & Yip Yio Chin Center for Stem Cell and Regenerative Medicine, School of Medicine, Zhejiang University

²Key Laboratory of Tissue Engineering and Regenerative Medicine of Zhejiang Province, School of Medicine, Zhejiang University

³State Key Laboratory for Diagnosis and Treatment of Infectious Diseases, Collaborative Innovation Center for Diagnosis and Treatment of Infectious Diseases, The First Affiliated Hospital, College of Medicine, Zhejiang University, Hangzhou, China

⁴Department of Sports Medicine, School of Medicine, Zhejiang university

⁵State Key Laboratory of High Performance Ceramics and Superfine Microstructure, Shanghai Institutes of Ceramics, Chinese Academy of Sciences, Shanghai 200050, China.

⁶Zhejiang University-University of Edinburgh Institute & School of Basic Medicine, Zhejiang University, Hangzhou, Zhejiang 310058, China

⁷China Orthopaedic Regenerative Medicine (CORMed)

⁸Department of Orthopaedics, The Second Affiliated Hospital, Zhejiang University School of Medicine, Hangzhou, Zhejiang, 310009, China

Corresponding author:

Center for Stem Cell and Tissue Engineering, School of Medicine, Zhejiang University, Hangzhou, Zhejiang, China

Tel: +86-571-88208442; Fax: +86-571-88208262

Email address: hwoy@zju.edu.cn (Hongwei Ouyang, MD, PhD)

Tel: +86-21-52412249, Fax +86-21-52413903

Email address: chentiewu@mail.sic.ac.cn (C. Wu)

Abstract

Osteochondral defects are most commonly characterized by damages to both cartilage and bone tissues as a result of serious traumas or physical diseases; because these two tissues have their own unique biological properties, developing a single monophasic scaffold that can concurrently regenerate these two specific lineages becomes a challenge. To address this concern, a silicon-based bioceramic (SiCP) scaffold was fabricated. The efficiency and underlying mechanisms of SiCP for osteochondral defect regeneration were investigated. At 8 and 16 weeks post-implantation in a rabbit model of osteochondral defect, gross morphology, histological, and micro-CT images showed that SiCP scaffolds distinctly promoted subchondral bone and cartilage regeneration when compared to calcium-phosphate based bioceramics (CP) scaffolds without silicon. *In vitro*, SiCP was also shown to promote bone marrow stem cells (BMSC) osteogenesis (*ALP*, *RUNX2*, *OCN*) and help maintain chondrocytes phenotype (*Acan*, *Sox9*, *Col2a1*), validated by qPCR, western blot, and RNA-sequencing (RNA-seq). Additionally, the descriptive analysis of RNA-seq using Gene Ontology (GO) and KEGG pathway analysis revealed biological processes related to cartilage and bone development and extracellular matrices in chondrocytes, as well as related to early osteogenesis in BMSC, indicating that Si ions play an important role in the regeneration of both tissues. Conclusively, the development of silicon-based bioceramic scaffolds may be a promising approach for osteochondral defect regeneration due to their unique dual-lineage bioactivity.

1. Introduction

Articular cartilage damages extending beyond into the subchondral bone layer are regarded as osteochondral defects. Even though the regeneration of these large defects has been extensively explored, it still presents a great challenge in orthopedic surgery due to the complicated osteochondral structure and poor self-repair capacity[1]. Osteochondral lesions typically lead to some spontaneous quick repair attempts where results are temporarily and only act to delay the degeneration process; the repaired defects are mainly filled with fibrous tissues, lack functional characteristics of natural hyaline cartilage, and are more susceptible to free radicals, metalloproteinases and catabolic cytokines[2,3]. Presently, the most common medical treatment methods for osteochondral defect repair are debridement, bone marrow stimulation techniques, and osteochondral grafts. While studies have demonstrated beneficial outcomes after

debridement and marrow stimulation, these effects are only palliative, not curative[4,5]. On the other hand, grafting techniques are retracted by several drawbacks relating to the necessity of secondary operation, inadequate amount of tissues that can be isolated, and also increased possibility of immune rejection and disease transmission [6,7]. Therefore, other potential alternative approaches must be developed for promoting osteochondral repair and regeneration, aiming at disease prevention and treatment instead of pain reduction.

Tissue engineering has emerged as one of the promising substitutes for tissue repair and regeneration. Current regenerative techniques, particularly autologous chondrocyte transplantation (ACT) and microfracturing, have been shown to effectively promote the restoration of joint surface cartilage[8–11]. However, because the majority of these approaches for osteochondral defect reconstruction was concentrated on the cartilage's upper layer while neglecting the lower subchondral tissue, most of the regeneration results were unsatisfactory [12]. Therefore, it is important to create a scaffold that could simultaneously regenerate these two lineages of osteochondral defects[13,14]. To overcome this obstacle, biphasic or bi-layered scaffolds have been created in an attempt to mimic the natural structure of cartilage and subchondral bone[15–18]. Although promising advancement has been achieved with this method, the crucial concern remains the inadequate resemblance of engineered cartilage and subchondral bone to the natural tissues, in terms of biomechanical characteristics, biochemical properties, and structural composition. Moreover, the fabricated bi-layered scaffold often suffers from insufficient bonding strength, possibly leading to the detachment of the two layers. Hence, developing a single scaffold that can biologically fulfill the requirements needed for simultaneously regenerating both the cartilage and subchondral bone is quite urgent.

Silicon (Si) has been extensively studied since Carlisle in the early 80's illustrating that Si promoted bone matrix synthesis[19]; this element is an important nutrient in the human body, playing a major part in healthy connective tissue including articular cartilage and bone. It was reported that Si had a positive influence on the regulation of cartilage extracellular matrix[20–22]. Furthermore, recent reports also revealed that Si promoted rat BMSC proliferation and differentiation, as well as enhanced osteoblasts' collagen synthesis process[23–26]. Based on the available reported scientific data, we hypothesized that silicate-based bioceramics can biologically fulfill the requirements for bi-lineage one-step (cartilage and subchondral bone) regeneration in osteochondral defects. However, even though Si have been illustrated to have

beneficial influences on chondrocytes and BMSCs, Si have not yet been extensively investigated for osteochondral defect repair.

In order to maximize the therapeutic effects of Si, a silicon-calcium-phosphate based bioceramic (SiCP) was successfully fabricated. Calcium phosphate bioceramics such as β -tricalcium phosphate (CP) and hydroxyapatite (HA), and calcium sulfate are commonly utilized as bone substitutes, due to their biological and physical similarity to the mineral portion of the native bone[27]. However, HA is limited by the slow degradation rate, hindering new bone formation and remodeling; thus, CP is more popularly used due to their biocompatibility and accessibility for osteochondral regeneration[28]. CP scaffolds possess highly inter-connected pores (200um-500um) similar to the subchondral bone porous structure. Considering the feasibility of dual-functional effects of silicate-based scaffolds on both bone tissue regeneration and cartilage preservation, Si-containing CP (SiCP) may further enhance osteochondral defect regeneration. Therefore, in this study, we aimed to fabricate a smart CP scaffold with sustained release of silicon ions. The efficiency of the scaffold in promoting regeneration of osteochondral defects was investigated in both *in vitro* cell culture and *in vivo* animal-based osteoarthritis model. Additionally, high throughput RNA-sequencing was also performed to reveal the overall transcriptomic fate of the cell population.

2. Methods

Preparation and characterization of scaffolds: Silicon-calcium-phosphate (SiCP, $\text{Si}_2\text{Ca}_7\text{P}_2\text{O}_{16}$) powders were synthesized by sol-gel process according to our previous publication[29]. For preparation of SiCP scaffolds, SiCP powders were added into 6% polyvinyl alcohol aqueous solution to form well-dispersed suspension with the ratio of 0.8 (powder/PVA mass). Porous polyurethan foam templates were immersed into the suspension and compressed with glass stick to force the suspension into the foams. After drying at 70°C, the composites were then sintered at 1400°C for 3 h to remove the polyurethan foam and form SiCP scaffolds. The pore structure of sintered scaffolds was observed by optical microscopy and characterized by X-ray diffraction (XRD) and scanning electron microscopy (SEM). For the control materials, β -calcium-phosphate (CP) scaffolds were fabricated with the same method as described above.

Ion release from SiCP and CP scaffolds: To assay different ion release from the SiCP and CP

scaffolds, both scaffolds were placed in DMEM medium (Gibco) for 7 days and the concentration of different ions released into the spent medium were determined by inductive coupled plasma atomic emission spectrometry (ICP-AES) (Perkin-Elmer Optima 7000DV).

Animal model of osteochondral defect: All animal models used in these studies were performed according to standard guidelines approved by the Zhejiang University Ethics Committee (#ZJU20170969). Adult male New Zealand white rabbits (weighted 2.5-3kg) were used for *in vivo* study. Under anesthesia with 1% pentobarbital sodium (40mg/kg), osteochondral cylindrical cartilage defects with 4mm in diameter and 5mm in depth were formed on the patellar groove with a stainless-steel punch on both the left and right limbs. Rabbits were randomized and divided into three groups: non-treated (blank, n = 8 joints), CP scaffolds (n = 8 joints), and SiCP scaffolds (n = 8 joints). Both CP and SiCP scaffolds were implanted into the defect groove before sterilization and wound closure while the non-treated group was simply sterilized and sutured. At 8 and 16-week post-surgery, rabbits were sacrificed and 7 knee joints from each group were histologically assessed.

Micro-CT image analysis of bones: Briefly, samples were fixed with 4% paraformaldehyde for 48 h. After image reconstruction, the desired region of interest with defects was assigned. The reconstructed images were then visualized and evaluated by Version 3.1 software provided by Shanghai Showbio (Biotech Co., Ltd, SKYSCAN 1076). Sample scanning related parameters are as follows: 70kv (voltage), 200uA (current), 30um (resolution), 300ms (exposure time).

Assessment of cartilage repair: At 8- and 16-week post-operation, rabbits were sacrificed by an intravenous overdose of pentobarbital. Seven samples from each group were collected, photographed, and blindly evaluated by four different investigators according to the International Cartilage Repair Society (ICRS) macroscopic assessment scale for cartilage repair[30]. Subsequently, serial sections (8-mm thick) were cut sagittally through the damaged site and stained with Safranin-O (Sigma). Repaired cartilages from different groups were blindly graded by 4 investigators, applying the ICRS Visual Histological Assessment Scale.

Cell isolation and culture: Human bone marrow mesenchymal stem cells (BMSCs) were obtained from bone marrow of patients undergoing femoral fracture surgery with their written consent, as approved by the ethics committee at the Second Affiliated Hospital of Zhejiang

University School of Medicine (study no.2016-033) and the First Affiliated Hospital of Zhejiang University School of Medicine (study no.2018-392). To isolate BMSCs, 3mL of bone marrow blood were suspended in 10mL complete culture media containing 10% fetal bovine serum (FBS) (Gibco) and 1% Penicillin-Streptomycin (P/S) (Gibco) before seeding them into 10cm dishes. When the cells attached and reached confluency, they were detached by 0.25% trypsin (Gibco) and re-suspended in supplemented DMEM media. BMSCs were maintained as a monolayer at 37 °C, the media were changed every 3 days; cells between 3rd to 5th passage were utilized for most experiments.

Primary mouse chondrocytes were isolated from the femoral condyles and tibial plateaus of postnatal day 0-1 C57B1/6 mice, as previously reported[31]. Briefly, isolated cartilages were washed with PBS containing 1% P/S before digestion with 0.2% collagenase-containing DMEM/F-12 media (Gibco) for 5-6 hours; cells were then spun at 1200 rpm for 5 minutes, re-suspended in new media, and plated. Chondrocytes were maintained as a monolayer in DMEM/F-12 supplemented with 10% FBS at 37 °C. Cells between 1st to the 3rd passage was utilized for experiments.

Cell proliferation assay: The Cell Counting KIT-8 (CCK-8) (Dojindo Molecular Technologies, Inc.) was applied to evaluate the proliferation of BMSCs and chondrocytes. Cells cultured in different media solutions for 0, 1, 3, and 5 days (DMEM/F-12, CP-supplemented DMEM/F-12, and SiCP-supplemented DMEM/F-12) were first incubated in 10% CCK-8 solution in a 5% CO₂ incubator at 37 °C for 2 h before the absorbance of the culture medium was measured at 450 nm. BMSCs and chondrocytes were cultured in growth medium containing different concentrations of dissolved CP and SiCP powder (0, 1.5625, 3.125, 6.25, 12.5, and 25mM) in order to evaluate their effects on cell proliferation.

Alizarin red staining: Briefly, human BMSCs were plated into a 24-well plate and cultured in osteogenic inductive media with different supplemented CP solutions (No-CP, CP, SiCP). After 14 days, cells were fixed with 4% (v/v) paraformaldehyde and stained with alizarin red (Selleck) (0.5%) before visualization with a light microscope (X7; Olympus, Tokyo, Japan). To quantify the results, cells were destained with a combination of 0.5 M HCL and 5% sodium dodecyl sulfate (SDS); absorbance of the extracted dye was measured at 405nm (TECAN).

qPCR analysis of gene expression: The mRNA transcript levels of osteogenic specific genes (*ALP*, *RUNX2*, and *OCN* (Generay biotechnology, Shanghai Generay Biotech Co.,Ltd)) within human BMSCs cultured in different supplemented osteogenic-inducing medium (control, CP, SiCP) were assessed by real-time PCR. Similarly, the mRNA transcript levels of chondrocyte specific genes (*Acan*, *Col2a1*, and *Sox9* (Generay biotechnology, Shanghai Generay Biotech Co.,Ltd)) within mouse chondrocytes cultured in different supplemented media were also assessed. In both cases, cells were harvested on day 3 then lysed in Trizol (Invitrogen Inc., Carlsbad, CA, USA) and mRNA was extracted according to the manufacturer's protocol. Reverse transcription was carried on using ReverTra Ace qPCR Master Mmix kit (TOYOBO, Japan) and PCR was performed using SYBR Green QPCR Master Mix (Takara) with a Light Cycler apparatus (Bio-rad, CFX-Touch). The PCR cycles consisted of 40 rounds of amplification of the DNA template with primers annealing at 60 °C; the relative expression level of each target gene was then calculated using the $2^{-\Delta\Delta Ct}$ method. The amplification efficiencies of primer pairs were validated to allow for quantitative comparison of gene expression. Each qPCR was done on at least 3 distinct experimental samples and representative outcomes were illustrated as target gene expression normalized to the reference gene GAPDH. Error bars represent one SD from the mean of technical replicates. The following primer sequences were applied: *ALP* sense 5'-CGGCCATCCTATATGGTAACGG-3', antisense 5'-CAGGAG GCA TACGCCATCACA-3'; *RUNX2* sense 5'-CCA ACTTCCTGTGCTCCGTG-3', antisense 5'-GTGAAACTCTTGCCCTCGTCCG-3'; *OCN* sense 5'-GACCCTCTCTC TGCTCACTCT-3', antisense 5'-GACCTTACTGCCCTC CTGCTTG-3'; *Acan-1* sense 5'-TGGTGATGATCTGGCACGAG-3', antisense 5'-CTCCGCTTCTGTAGTCTGCG-3'; *Col2a1* sense 5'-GACCCCATGCAGTACATG-3', antisense 5'-GACGGTCTTGCCCCACTT-3' and *Sox9* sense 5'-CACACTACAGCCCCCTCCTAC-3', antisense 5'-CCTCCTCAAGGTCGAGTGAG-3'.

Western blot analysis: To quantify protein expression levels of type II collagen, SOX9, and GAPDH in mouse chondrocytes, as well as RUNX2 and GAPDH in human BMSCs (abcam), cytosolic proteins of these cells were directly extracted with radio immune precipitation assay (RIPA) lysis buffer combining with a cocktail of protease and phosphatase inhibitor. The total extracted protein concentration was calculated using the BCA Protein Assay Kit (Pierce #23227).

The proteins were then separated on SDS-PAGE gels before transferring the gel onto a polyvinylidene difluoride membrane; after the transfer process, the membrane was blocked in 1% (w/v) BSA for 1h at room temperature and incubated overnight at 4 °C with the appropriated primary antibodies. PBS with Tween (PBST)(Sangon Biotech) was then used to wash the membrane before incubation with the diluted HRP-conjugated secondary antibody (1:1500)(Beyotime Biotechnology) for 2 h at room temperature. The excess secondary antibody was rinsed off again with PBST, and subsequently western blot detection reagents (ECL, Beyotime Biotechnology) were utilized according to the manufacturer's instructions to generate chemiluminescent signal.

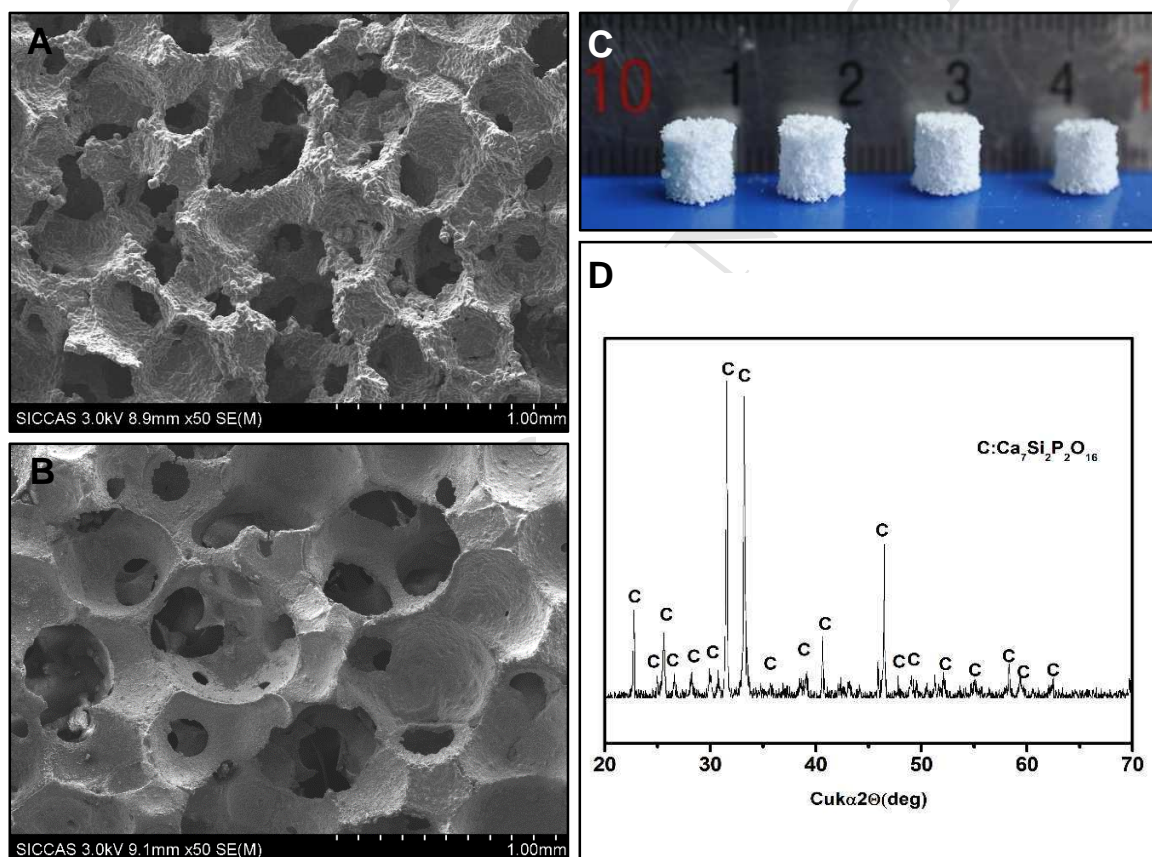
RNA-seq and data analysis: RNA-seq was modified from a previous method[32]. In brief, total RNA was extracted from tissue samples using Trizol reagent (TAKARA), reverse transcription was conducted by SuperScript II reverse transcriptase (Invitrogen), double strand cDNA was conducted using NEBNext mRNA second strand synthesis kit (NEB), double strand DNA was cleaned with AMPure XP beads (Beckman Coulter), sequencing library was constructed with Nextera XT kit(Illumina) and sequenced on Illumina X-Ten platform. Sequence reads were mapped to reference genome mm10 using Bowtie2 with default parameters, and per gene counts were calculated using HTSeq[33]. All the statistical analyses were conducted using R statistical programming language. We used DESeq2 to identify differentially expressed genes [14]. In our analyses, a gene was considered to be expressed in a sample if its count value was equal or greater than 1 in the sample. Differentially expressed genes (DEGs) were defined as foldchange ≥ 2 and p-value ≤ 0.05 . Heatmaps were generated with pheatmap package[34]. Gene ontology analysis was performed using DAVID and REVIGO (<https://david.ncifcrf.gov>; <http://revigo.irb.hr/>). For each group, 4 duplicates were collected and their RNAs were extracted, sequenced, and analyzed.

Statistical analysis: All data are presented as mean \pm standard deviation (SD). One-way analysis of variance (ANOVA) and Student's t-test were applied to calculate the differences between values. Values of $p < 0.05$ were considered to be statistically significant; level of significance presented as * ($p < 0.05$), and ** ($p < 0.01$).

3. Results

3.1 Characterization of porous SiCP scaffolds

The gross structure and morphology of the scaffolds are shown in figure 1. The resulting scaffolds were examined by scanning electron microscopy (SEM). SEM images illustrated that SiCP scaffolds had a highly inter-connective porous structure with diameters ranging from 200-500 μm (Fig 1A, C); CP scaffolds were also illustrated to have an interconnected porous structure (Fig. 1B). Figure 1D shows the diffraction patterns of X-rays for SiCP scaffolds with pure $\text{Si}_2\text{Ca}_7\text{P}_2\text{O}_{16}$ crystal phase (JCPD: 11-0676). The release profile of different ions from the SiCP and CP scaffolds were also investigated; both scaffolds were placed in DMEM medium



and the concentration of silicate released was analyzed using ICP-AES (FigS1).

Figure 1: The microstructural and biological characteristics of SiCP scaffolds. SEM images of (A) SiCP and (B) CP scaffolds at high magnification. (C) Optical images of the whole SiCP scaffolds, 1mm scale bars. (D) XRD analysis for SiCP scaffolds.

3.2 In-vivo evaluation of SiCP scaffolds for osteochondral defect repair

3.2.1 SiCP scaffold for osteochondral defect repair in a rabbit model

SiCP scaffolds were then evaluated for osteochondral defect repair in a rabbit model; either CP or SiCP scaffolds were implanted into the created defect groove as shown in figure 2A, the control had no scaffold implantation. At 8 weeks, no inflammatory reaction was detected in all groups, indicating good *in vivo* biocompatibility of scaffolds; however, defects in the non-treated and pure CP groups were filled with diseased and friable tissue. The non-treated group showed the slowest formation of new tissues, with the defect surface still exposed; CP group showed a smaller area of unorganized and incomplete tissue formation when compared to the non-treated group, while glossy white and well-integrated tissue was observed in the SiCP group (Fig 2B). At 16 weeks after surgery, the gross results for all three groups were superior when compared to results from week 8; the defected area of both the non-treated and CP groups was significantly reduced, but still with some visibility of previous injuries, while a smooth well-integrated surface was observed in the SiCP group. According to the ICRS scores, the average scores in both the pure CP and SiCP groups were significantly higher when compared to the non-treated control group, with the SiCP group having the highest average scores at both 8- and 16-week (Fig 2C).

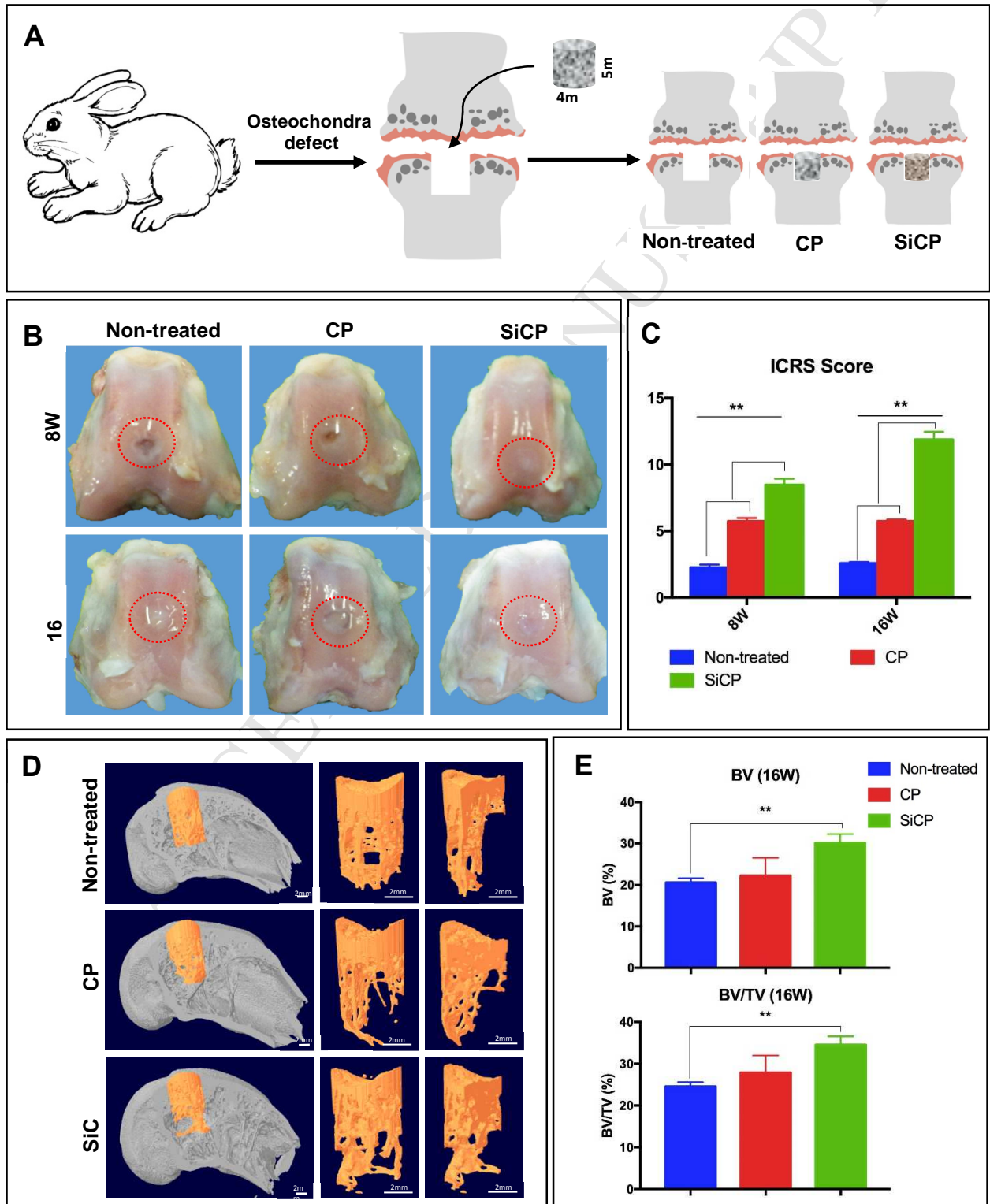


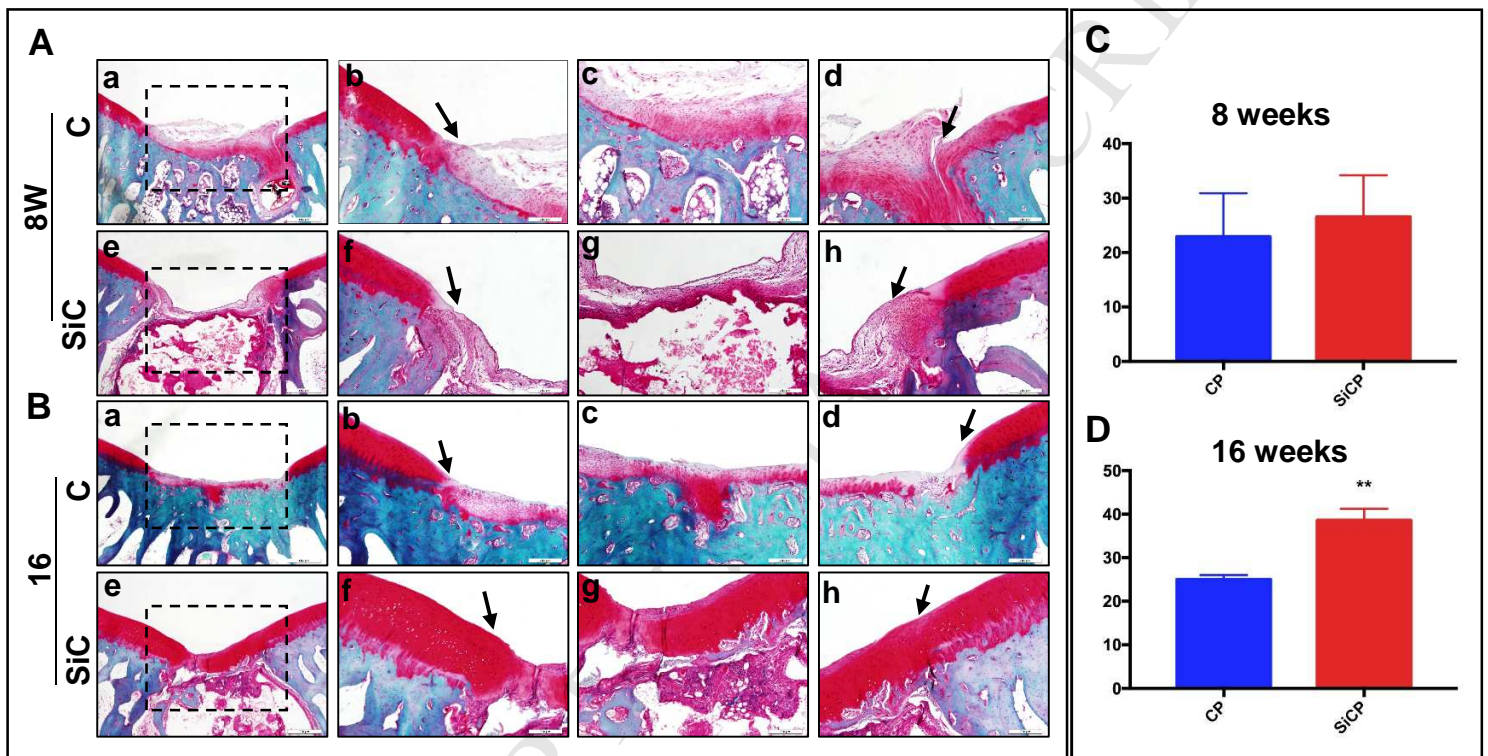
Figure 2: Comparison of *in vivo* osteochondral defect repair in three experimental groups at 8 (8W) and 16 weeks (16W) post-surgery. (A) Schematic diagram of the experimental design and procedure. (B) Gross images illustrating osteochondral defects in three groups (non-treated, CP, SiCP) at 8 (upper) and 16 (lower) weeks. (C) ICRS scores for the three different groups at 8 and 16 weeks post-surgery. (D) 3D micro CT images of subchondral bone in three groups and (E) a quantitative analysis for new bone formation including BV (bone volume) and BV/TV (bone volume/tissue volume) at 16 weeks post-surgery. ICRS, International Cartilage Repair Society. * $P < 0.05$, ** $P < 0.01$.

To further examine the *in vivo* stimulatory effects of SiCP scaffolds, Micro-CT scans were also conducted at 16-week post-implantation, where the defect regions implanted with SiCP scaffolds demonstrated much more calcified tissue when compared to other groups (Fig 2D). Three-dimensional reconstruction images illustrated that nascent bone tissues in the SiCP group filled around and within the whole defect region, whereas nascent bone tissues in the non-treated and CP group only partially filled the side or the upper level of the defect area (Fig 2D). In addition, the calculated bone volume (BV) and relative bone volume fraction (BV/TV) of the SiCP group were significantly higher than the control group when compared to the pure CP group at week 16 (Fig 2E). Thus, these data illustrated that SiCP enhanced the repair of osteochondral defect, exhibiting to be more superior to both the non-treated and pure CP groups.

3.2.2 The preservation of cartilage tissue by SiCP scaffold *in vivo*

Since the *in vivo* osteochondral defect repair model illustrated that CP and SiCP scaffolds were both quite effective in promoting the healing process when compared to the non-treated group, we further evaluated the efficacy of SiCP, comparing with pure CP, for osteochondral defect repair with Safranin-O staining in order to determine its ability to preserve and repair cartilage tissue. At 8 weeks post-implantation, the joint surface of the defect was filled with a mixture of fibrous and cartilage-like tissue in the CP group, neo-bone formation was also observed in the subchondral space (Fig 3Aa-d). Similarly, a large amount of hyaline-like cartilage was detected in the SiCP group, with some neo-bone formation in the subchondral space (Fig 3Ae-h). However, the difference between the two groups was not significant at 8 weeks post-implantation as illustrated by the mean ICRS histological score (Fig 3C). After 16 weeks, the defect in the CP group was almost covered with a mixture of hyaline cartilage-like tissue as well as fibrous tissue (Fig 3Ba-d); neo-bone was also detected in the CP group.

Remarkably, the SiCP group exhibited a more superior and thicker hyaline cartilage-like tissue formation, bridging over the defect, suggesting the facilitating effect of silicate-based ions on cartilage maintenance and repair. The mean ICRS histological score was approximately 1.5 times higher in the SiCP group when compared to the CP group (Fig 3D) ($P < 0.01$). Thus, the superior regeneration speed and quality of the regenerated cartilage and subchondral bone in the Si-incorporated CP scaffold, combined with Micro-CT three-dimensional reconstruction and



quantitative analysis, indicated that silicate-based ions released by the CP scaffold were capable of promoting both subchondral bone repair and cartilage regeneration.

Figure 3: Histological evaluation at 8 and 16 weeks post-operation. Histological sections at (A) 8 and (B) 16 weeks post-operation were visualized in two groups: (Aa-d, Ba-d) CP and (Ae-h, Be-h) SiCP. (A, B (a,e)) Original magnification x40; scale bar: 500 mm. (A,B (b-d,f-h)) magnification x100; scale bar: 200mm. (C-D) ICRS scoring on repaired cartilage at 8 and 16 weeks post-operation. The edge of the defect is indicated with a black arrow. * $P < 0.05$, ** $P < 0.01$.

3.3. In-vitro evaluations of SiCP for osteochondral defect repair

3.3.1 Underlying mechanism of SiCP scaffold in promoting bone repair

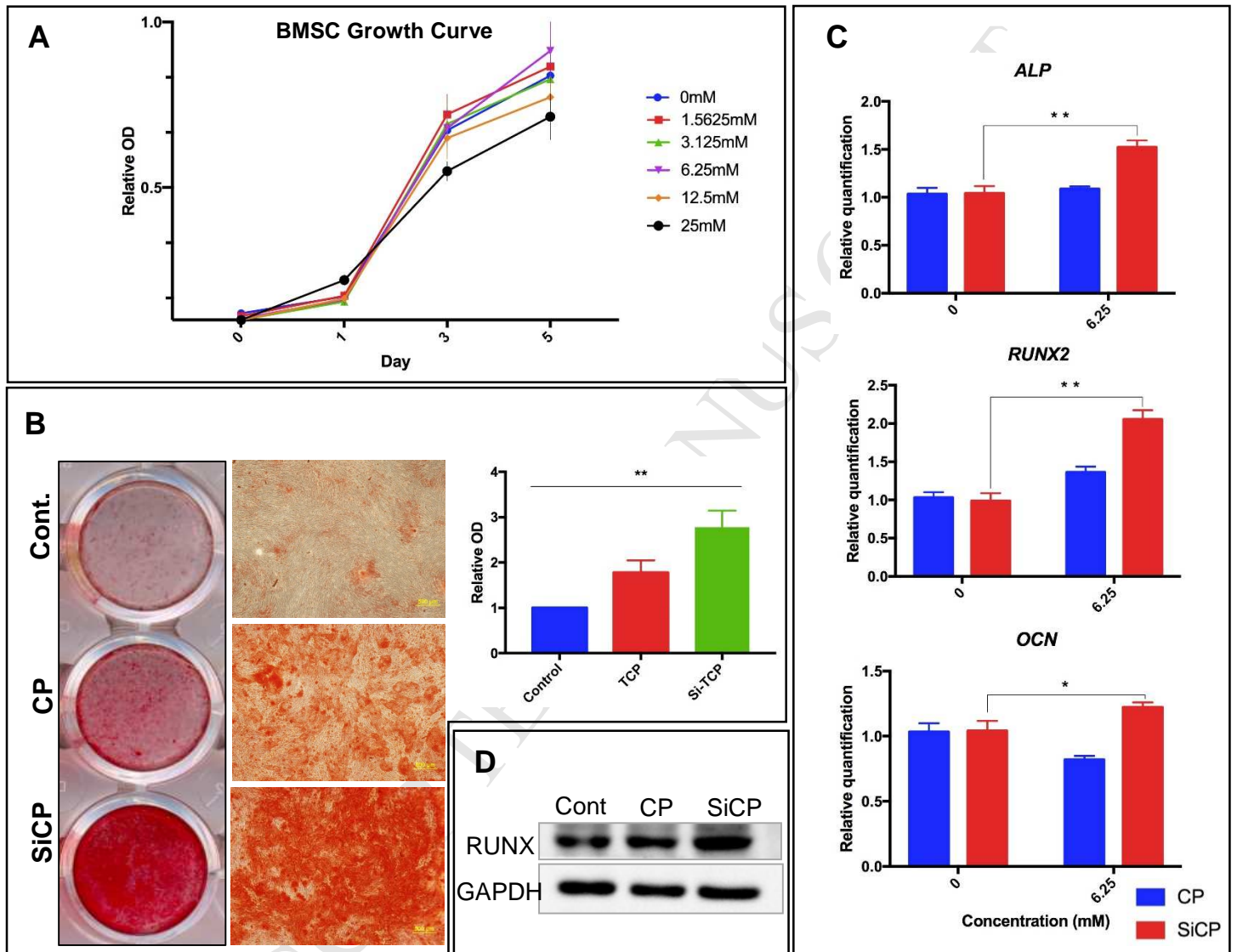


Figure 4: The effects of SiCP-added media on human BMSCs' osteogenic induction. (A) BMSC proliferation was examined in a range of SiCP concentrations with CCK8 to determine the best concentration for in vitro studies. (B) Alizarin Red staining was utilized to visualize the impact SiCP on osteogenesis of BMSCs. (C) Osteogenesis-related gene expressions (*ALP*, *RUNX2*, and *OCN*) in BMSCs cultured in SiCP and CP extracts. (d) *RUNX2* and *GAPDH* protein expression levels in BMSCs cultured with the two different media were also assessed by Western blot. * $P < 0.05$, ** $P < 0.01$. (Cont = control, BMSC = bone marrow mesenchymal stem cell)

The mechanisms of SiCP scaffold in promoting bone formation and repair was further evaluated with human BMSC (hBMSC) culture model. CCK-8 analysis revealed that BMSCs were able to proliferate in both high and low concentrations of SiCP (1.5625mM to 25mM) (Fig4A), with 6.25 mM being the optimal concentration. A range of SiCP concentrations was also tested on BMSC osteogenesis in order to further confirm the optimal concentration, since the CCK-8 result was not so obvious; qPCR and western blot results illustrated that SiCP at the concentration of 6.25 mM promoted osteogenic differentiation when compared to other concentrations (FigS2). Therefore, we carried on using the concentration of 6.25 mM to evaluate the effect of SiCP on hBMSC osteogenesis, which was visualized by alizarin red staining and quantified by optical density (OD) measurement at 405 nm. The obtained results illustrated that the incorporation of SiCP into osteogenic inductive media significantly enhanced BMSC osteogenic differentiation when compared to the CP and control group (Fig4B). The calculated OD value at 6.25 mM SiCP concentration markedly increased by 2.75 fold ($p<0.001$) when compared to the control group, and by 1.54 fold ($p<0.05$) compared to the CP group. Taken together, our results indicated that the addition of SiCP into the media promotes proliferation and osteogenic differentiation of BMSCs.

Gene expression of BMSCs in the osteogenic inductive culture was also evaluated with qPCR (Fig 4C); results showed the expression of *ALP*, *RUNX2*, and *OCN* genes were significantly upregulated after culturing in SiCP-added media for 3 days when compared to other groups (Fig 4C). Protein expression of BMSCs was also evaluated using western blot, illustrating an increased expression of *RUNX2* as compared to the CP and control group, thus suggesting that silicate-based ions enhance the osteogenic differentiation of BMSCs.

3.3.2 Mechanisms of SiCP scaffold in cartilage tissue protection

Similarly, CCK-8 was also first performed in the mouse chondrocyte culture model to evaluate the effect of SiCP on cartilage tissue preservation. CCK-8 analysis revealed that chondrocyte proliferation at a relatively low concentration range of SiCP (lower or at 6.25mM) had a quantifiable increment over time, whereas cell proliferation was repressed at higher concentrations of SiCP (12.5 and 25mM), noticeably after day 3 (Fig 5A). Thus, overall, our results suggested that 6.25mM is the optimal SiCP concentration in promoting chondrocyte proliferation.

To examine the influence of SiCP on chondrocytes' phenotype maintenance, we analyzed gene expression of chondrocytes in the SiCP-incorporated chondrogenic culture condition. Results illustrated that the expression of chondrocyte-related genes *Acan*, *Col2a1*, and *Sox9* in chondrocytes cultured in SiCP were significantly upregulated when compared to the control and CP media group (Fig 5C). Western blot results also showed significantly increased expression of SOX9 and COL2A1 in chondrocytes cultured in SiCP-added media as compared to CP media (Fig 5B).

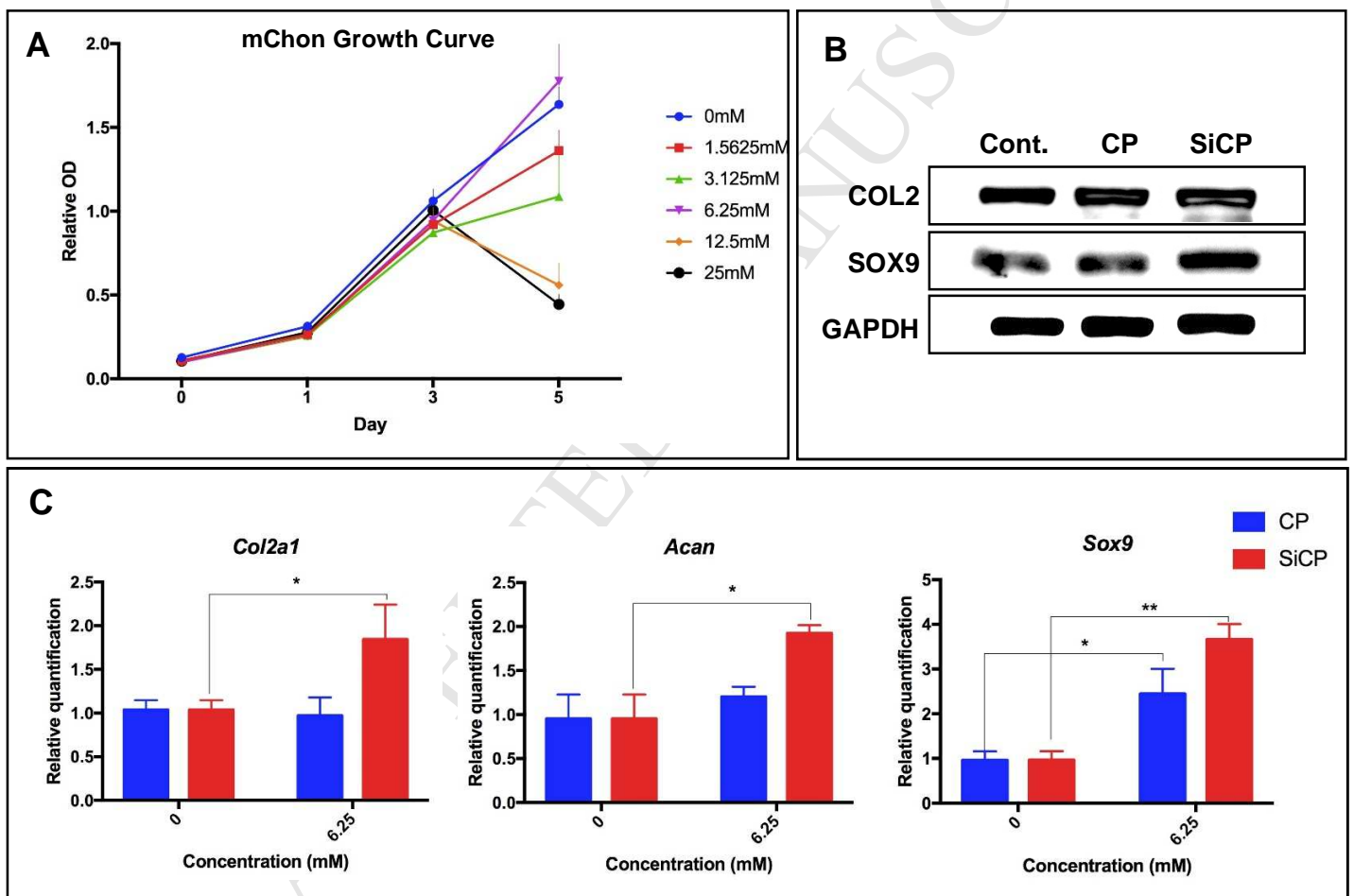


Figure 5: The effects of SiCP-added powder on mouse chondrocytes. (A) Mouse chondrocyte proliferation was examined in a range of SiCP concentrations with CCK8 to determine the best concentration for in vitro studies. (B) COL2A1, SOX9, and GAPDH protein expression levels in chondrocytes cultured with the two different media were also assessed by Western blot. (C)

Chondrocyte-related gene expressions (*Col2a1*, *Acan*, and *Sox9*) in mouse chondrocytes cultured in SiCP and CP extracts. * $P < 0.05$, ** $P < 0.01$. (Cont = control, mChon = mouse chondrocytes).

3.3.3 SiCP influences gene expression patterns of hBMSC and chondrocytes

To further confirm the obtained results on the transcriptomic scale, whole transcriptome RNA sequencing was also performed on the cells cultured in different media solutions. In hBMSC samples, 715 DEGs, including 377 upregulated and 338 downregulated genes were obtained in the CP group (Fig6A). By contrast, 811 DEGs were identified in the SiCP group, comprising of 495 upregulated and 406 downregulated genes (Fig6A). Venn diagram showed that the overlapping upregulated and downregulated genes between the two groups in hBMSCs were 124 and 62 respectively. In mouse chondrocytes, 858 DEGs, with 449 upregulated and 409 downregulated genes, were identified in the CP group while 926 DEGs, including 451 upregulated and 475 downregulated genes were obtained in the SiCP group (Fig6A). The overlapping upregulated and downregulated genes between CP and SiCP groups are also illustrated in the diagram, with 80 and 75 genes overlapped respectively. Heatmaps comparing DEGs induced in human BMSCs (Fig6Ba) and mouse chondrocytes (Fig6Bb) in response to CP-power and SiCP-power media additives are shown. Results demonstrated significant changes in the transcriptomic profile when cultured in CP and SiCP-powder-added media; the heatmap clustering based on the genes with p -value < 0.05 and \log_2FC above or below cutoff (>1 , <-1) showed that different added power induced a unique overall response (Fig6B). Volcano plots of the upregulated and downregulated DE genes in chondrocytes and hBMSCs (SiCP vs. Control; SiCP vs. CP) are illustrated in supplementary data (FigS2).

To further obtain functional insights, the gene ontology (GO) enrichment analysis was executed (Fig6C; FigS4). Results showed that GO terms of chondrocytes cultured in SiCP-added media were prominently related to cartilage development and regulation of bone mineralization, extracellular matrix, and positive regulation of collagen biosynthetic process (Fig6C); thus suggesting the preservation of chondrocytes' phenotype. Furthermore, we observed that there was also an enrichment in GO terms associated with cartilage/bone cellular functions and proliferation including regulation of growth, regulation of calcium ion transport, cellular iron ion homeostasis, and cellular zinc ion homeostasis. The GO result also suggests that the SiCP is non-toxic to chondrocytes, demonstrated by the enrichment of GO terms relating to negative

regulation of inflammatory response, cell death, and apoptotic process, thus further validating the CCK-8 results.

GO term enrichment analysis was similarly performed in human BMSCs culture in both CP-added and SiCP-added osteogenic media. Most of the enriched biological processes are related to protein binding, response to mechanical stimuli, cell division, and cell proliferation (Fig 6C); these biological processes have previously been reported in other works concerning early MSC osteogenic induction[35,36]. Furthermore, data on hBMSCs cultured in SiCP-added media showed GO clusters related to “actin cytoskeleton organization”, “embryonic skeletal system development”, as well as “Wnt signaling pathway, planer cell polarity pathway”. Taken together, our results illustrate that the incorporation of SiCP helps to maintain chondrogenic phenotype markers and promoted the initiation of MSC osteogenesis.

A KEGG pathway analysis in the upregulated gene group was also carried out using DAVID. The top pathways of upregulated genes for the two cell types are shown in figure 6D. The “Cell cycle” KEGG pathway was greatly induced during BMSC osteogenesis; previous observations reported an increase in cell proliferation during osteogenesis, thus supporting this outcome[37]. In mouse chondrocytes, our results showed that an important pathway in chondrocyte phenotype preservation is the “TGF-beta signaling pathway”, which is consistent with other reports demonstrating positive effects of TGF-beta signals in the maintenance of articular cartilage[38,39].

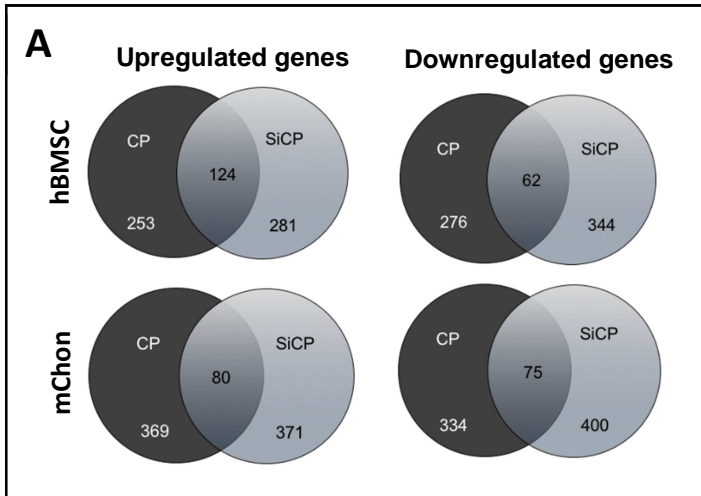
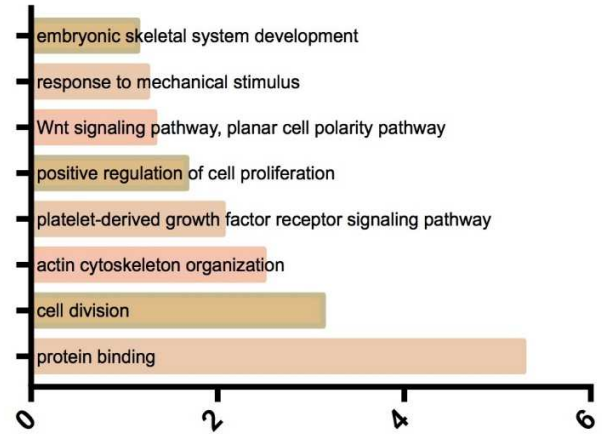
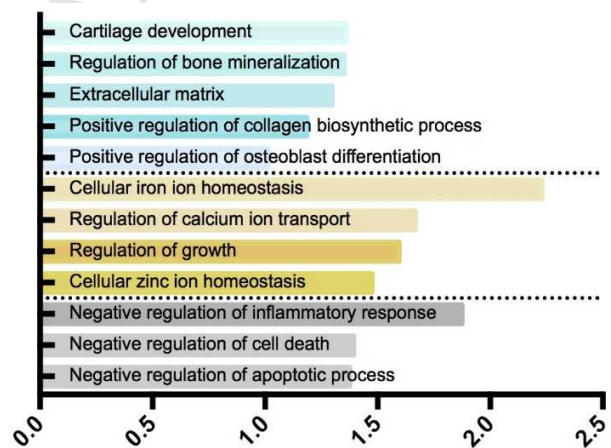
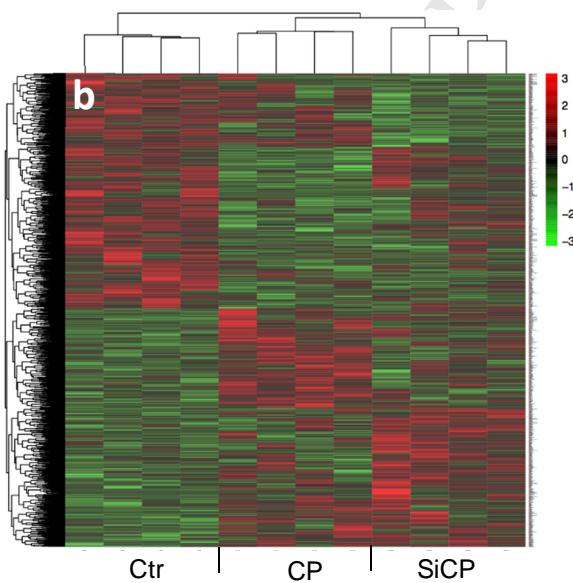
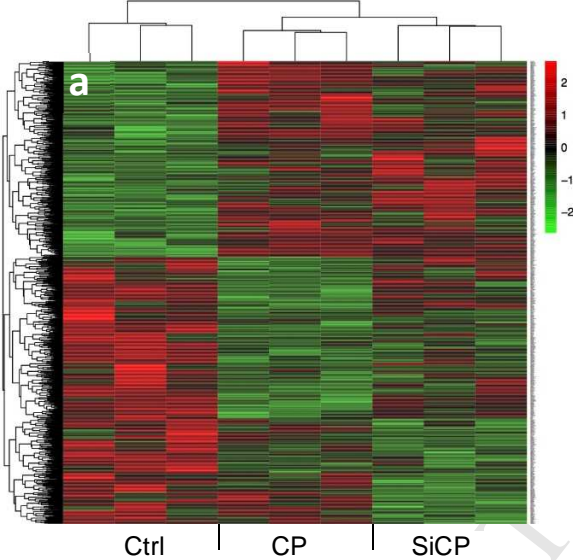
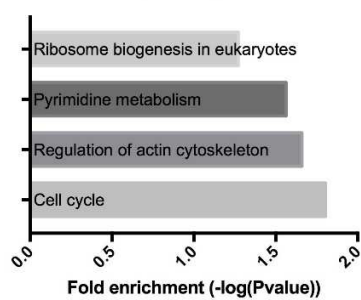
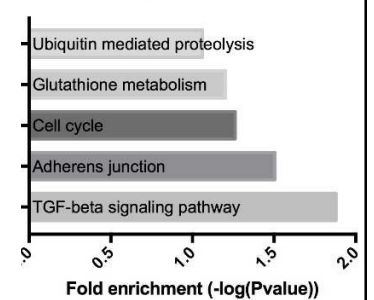
**C****GO Analysis: SiCP on****GO Analysis: SiCP on mChon****B****KEGG pathway: hBMSC****KEGG pathway: mChon**

Figure 6: A whole transcriptome RNA-sequencing of hBMSCs and mChons. (A) The number of significantly altered genes (≥ 2 -fold difference: upregulated and downregulated) after cultured in CP and SiCP extracted media is illustrated. (B) A Heatmap of differentially expressed mRNA levels from RNA-seq analysis performed on (a)hBMSCs and (b)mChons. (C) Gene Ontology (GO) enrichment analysis of the relevant upregulated genes in hBMSC (top bar chart) and mChon (bottom bar chart). (D) The results from the KEGG pathway analysis through DAVID are illustrated within the category of upregulated genes after cultured with SiCP extracts in both cell types.

Discussion

SiCP scaffolds were successfully developed, and were illustrated to enhance osteochondral defect regeneration. As mentioned, the optimal strategy for osteochondral defect repair is not only due to the restoration or preservation of only the cartilage layer but also the underlying subchondral bone[40,41]. The current study revealed that silicate-based bioceramic scaffolds could successfully promote repair of two different differentiated tissues *in vivo* (cartilage and bone) and growth and maintenance of two types of differentiated cells (osteoblasts differentiated from BMSCs and chondrocytes).

First, the repair efficacy of scaffolds was tested *in vivo*; the histological analysis and Micro-CT results indicate that SiCP scaffolds significantly promote osteochondral defect repair, simultaneously enhancing bone regeneration and preserving hyaline cartilage-like tissues, as compared to CP scaffolds, the most common standard bio-ceramic scaffolds for bone regeneration. We also evaluated the effects of the released silicate-based ions on BMSCs and chondrocytes, where results suggested that SiCP promoted osteogenic differentiation of BMSCs and maintained the phenotype of chondrocytes *in vitro*. In mouse chondrocytes, pure CP extracted were shown to promote chondrogenic genes expression, which is consistent with previous reports[42–44]. However, SiCP extracts significantly elevated *Acan*, *Sox9*, and *Col2a1* production when compared to cells that were simply cultured in CP extracts; this outcome was further validated with western blot. Similarly, SiCP extracts also significantly enhanced osteogenic gene expression markers *ALP*, *RUNX2*, and *OCN*. Additionally, BMSCs cultured in SiCP extract showed a more intense ARS staining when compared to control and CP extract groups, indicating greater cell mineralization.

The whole transcriptomic profile of mouse chondrocytes and human BMSCs cultured in the SiCP-incorporated media was also evaluated. The analyzed data demonstrated that cells cultured in different media had differential gene expression profiles. When compared to the

control group, the SiCP-incorporated media group showed GO terms related to cartilage and bone development, as well as negative responses to inflammatory responses and apoptosis in mouse chondrocytes. Additionally, GO terms including “extracellular matrix” and “positive regulation of collagen biosynthetic process” elements dominated in the human articular cartilage, were also observed. Cartilage-related GO terms indicated that mouse chondrocytes cultured in media with SiCP were superior in maintaining the original chondrocyte phenotypes and characteristics. Moreover, in mouse chondrocytes, KEGG pathway analysis showed enrichment for TGF-beta signaling pathway. TGF-beta was previously reported to be essential for the development of chondrocytes and protection against osteoarthritis [39,45,46]; thus, these data suggested that SiCP may enhance cartilage/bone repair through the TGF-beta signaling pathway. However, conversely, because TGF-beta has also been shown to be associated in ageing and OA cartilage degeneration depending on the alternative stimulation of other signaling pathways[47–49], more research is needed to accurately decipher the exact mechanism of SiCP in cartilage repair.

For human BMSCs, other than the GO term “embryonic skeletal system development, our GO enrichment analysis did not reveal strong key terms related to MSC osteogenesis; however, we found upregulated gene sets related to early osteogenic induction such as *SEMA3A* (Semaphorin 3A), and *HOXA9* (FigS3). Semaphorins (Semas) are a huge family of conserved regulator proteins that modulate cellular shape and function[50]. *SEMA3A*, or a member of class 3 Semas, has recently been reported to play crucial roles in bone metabolism; over-expression of *SEMA3A* has been shown to increase cell proliferation, speed up MSCs’ ossification process, and enhance osteogenic marker gene expressions[51,52]. On the other hand, *HOXA9* gene encodes transcription factors that regulate skeletal patterning in the developing embryo; numerous studies also stated that *HOX* genes continue to be expressed in mature bones and function during the healing process after fracture injuries[53–55]. Interestingly, the upregulated GO term in human BMSCs also consisted of Wnt signaling pathway (GO:0060071 Wnt signaling pathway, planar cell polarity pathway); the cell polarity pathway is one of the main noncanonical Wnt pathways responsible for the regulation of cytoskeletons through the activation of GTPases[56,57]. *Okamoto et al.* reported that the noncanonical ligand Wnt 5a suppressed PPAR-gamma function, thus inducing osteogenic differentiation of MSCs[58,59]. It was also previously reported that Si stimulated MSCs differentiation by activating Wnt pathways [44,60]; therefore, it is reasonable

to hypothesize that Si ions released from SiCP scaffold may help to promote MSC osteogenic induction and subchondral bone regeneration through Wnt signaling pathway.

However, we recognize some limitations of this study; first, the follow-up period in the rabbit model of osteochondral was relatively short, thus limiting our knowledge on the possible long-term effects of SiCP scaffolds *in vivo*. Furthermore, not limiting to merely the joint environment, we realize that there might be some possible influence on other body parts and systems after scaffold implantation; thus, a whole-body systemic evaluation after scaffold implantation will be carried out in the near future. Biomechanical assessment of the repair cartilage was also not performed; therefore, future studies should also include the evaluation of biomechanical properties of repaired cartilage as this is essential for functional cartilage restoration. Moreover, despite improved tissue formation observed via histological analysis, evaluation and observation of the live subjects' behaviors and responses to the implanted materials should also be performed in order to further and completely demonstrate the SiCP scaffold' ability to facilitate osteochondral defect repair and its influence on the tested subjects. Lastly, even though our RNA-seq data showed supportive information validating our *in vitro* results, further studies will be carried out in the future to further confirm the signaling pathways involved.

As mentioned, articular osteochondral defects resulted from trauma or bone diseases are often observed to be accompanied by defects of the subchondral bone[61]. Tissue engineering provides a novel approach for cartilage repair, but it is a complicated procedure involving interactions between the scaffold construct, the seeded cells, and multiple cytokines. Numerous scaffold designs have been generated for osteochondral defect repair, including bi-phasic scaffolds and other multilayered scaffolds. However, as mentioned, these designs could not biologically and accurately mimic the native osteochondral tissue's structure; additionally, the bonding strength of the bi-layered scaffold may not be sufficient enough, thus leading to the separation of the two layers. There are few reports that utilized a single scaffold for osteochondral regeneration, promoting both the repair of subchondral bone and cartilage. Here, a single dual-lineage SiCP scaffold was fabricated and applied to repair osteochondral defects *in vivo*. The monophasic structure of SiCP scaffolds could eliminate problems associated with multilayered scaffolds. *In vitro* studies suggest that it is possible that SiCP promotes human BMSC osteogenesis by activating the Wnt pathway, and further helps maintain chondrocyte

phenotypic characteristics via the TGF-beta signaling pathway.

Conclusion

Conclusively, SiCP scaffolds were successfully created, enabling the release of Si ions *in situ*. The release of Si ions showed positive effects in promoting BMSC osteogenesis and preserving chondrocytes from dedifferentiation, simultaneously enhancing cartilage and subchondral bone regeneration. A whole transcriptome RNA-sequencing suggested that monophasic SiCP scaffolds possess dual-lineage ability for regeneration of both the cartilage and subchondral bone, providing options for the use of bioactive ions for osteochondral defect repair.

Acknowledgment

Funding for this study was supported by National Key Research and Development Program of China (2016YFB0700804), NSFC grants (81630065, GZ1094, 81472115, 81672162), and Science and Technology Commission of Shanghai Municipality (17441903700).

Appendix A. Supplementary data

The following is the supplementary data related to this article:

Supporting Information (SI): Figures S1-S4

Author Disclosure Statement

No competing financial interests exist.

Data availability

The raw/processed data required to reproduce these findings cannot be shared at this time as the data also forms part of an ongoing study.

Reference:

- [1] L.Z. Zhang, H.A. Zheng, Y. Jiang, Y.H. Tu, P.H. Jiang, A.L. Yang, Mechanical and biologic link between cartilage and subchondral bone in osteoarthritis, *Arthritis Care Res.* 64 (2012) 960–967. doi:10.1002/acr.21640.
- [2] M. Lotz, Cytokines in cartilage injury and repair, in: *Clin. Orthop. Relat. Res.*, 2001. doi:10.1097/00003086-200110001-00011.
- [3] S. Panseri, A. Russo, C. Cunha, A. Bondi, A. Di Martino, S. Patella, E. Kon, Osteochondral tissue engineering approaches for articular cartilage and subchondral bone regeneration, *Knee Surgery, Sport. Traumatol. Arthrosc.* (2012) 1182–1191. doi:10.1007/s00167-011-1655-1.
- [4] A.W.A. Baltzer, C. Moser, S.A. Jansen, R. Krauspe, Autologous conditioned serum (Orthokine) is an effective treatment for knee osteoarthritis, *Osteoarthr. Cartil.* 17 (2009) 152–160. doi:10.1016/j.joca.2008.06.014.
- [5] S.-F. Sun, Y.-J. Chou, C.-W. Hsu, W.-L. Chen, Hyaluronic acid as a treatment for ankle osteoarthritis., *Curr. Rev. Musculoskelet. Med.* 2 (2009) 78–82. doi:10.1007/s12178-009-9048-5.
- [6] P. V. Giannoudis, H. Dinopoulos, E. Tsiridis, Bone substitutes: An update, *Injury.* 36 (2005) S20–S27. doi:10.1016/j.injury.2005.07.029.
- [7] O. Arosarena, Tissue engineering., *Curr. Opin. Otolaryngol. Head Neck Surg.* 13 (2005) 233–241. doi:10.1097/01.moo.0000170526.51393.c5.
- [8] J. Freitag, D. Bates, R. Boyd, K. Shah, A. Barnard, L. Huguenin, A. Tenen, Mesenchymal stem cell therapy in the treatment of osteoarthritis: Reparative pathways, safety and efficacy - A review, *BMC Musculoskelet. Disord.* 17 (2016) 1–13. doi:10.1186/s12891-016-1085-9.
- [9] H. Chiang, T.F. Kuo, C.C. Tsai, M.C. Lin, B.R. She, Y.Y. Huang, H.S. Lee, C.S. Shieh, M.H. Chen, J.A.M. Ramshaw, J.A. Werkmeister, R.S. Tuan, C.C. Jiang, Repair of porcine articular cartilage defect with autologous chondrocyte transplantation, *J. Orthop. Res.* 23 (2005) 584–593. doi:10.1016/j.orthres.2004.11.003.
- [10] J.R. Steadman, K.K. Briggs, J.J. Rodrigo, M.S. Kocher, T.J. Gill, W.G. Rodkey, Outcomes of microfracture for traumatic chondral defects of the knee: Average 11-year follow-up, *Arthrosc. - J. Arthrosc. Relat. Surg.* 19 (2003) 477–484. doi:10.1053/jars.2003.50112.

- [11] L. Hangody, P. Fules, P. Füles, Autologous osteochondral mosaicplasty for the treatment of full-thickness defects of weight-bearing joints: ten years of experimental and clinical experience, *J Bone Jt. Surg Am.* 85–A Suppl (2003) 25–32. doi:10.1002/1529-0131(199808)41:8<1331::aid-art2>3.0.co.
- [12] E.B. Hunziker, The elusive path to cartilage regeneration, *Adv. Mater.* 21 (2009) 3419–3424. doi:10.1002/adma.200801957.
- [13] T. Muraoka, H. Hagino, T. Okano, M. Enokida, R. Teshima, Role of subchondral bone in osteoarthritis development: A comparative study of two strains of guinea pigs with and without spontaneously occurring osteoarthritis, *Arthritis Rheum.* 56 (2007) 3366–3374. doi:10.1002/art.22921.
- [14] Y. Henrotin, L. Pessesse, C. Sanchez, Subchondral bone and osteoarthritis: Biological and cellular aspects, *Osteoporos. Int.* 23 (2012) 847–851. doi:10.1007/s00198-012-2162-z.
- [15] X. Li, J. Ding, J. Wang, X. Zhuang, X. Chen, Biomimetic biphasic scaffolds for osteochondral defect repair, *Regen. Biomater.* (2015) 221–228. doi:10.1093/rb/rbv015.
- [16] I. Schleicher, K.S. Lips, U. Sommer, I. Schappat, A.P. Martin, G. Szalay, S. Hartmann, R. Schnettler, Biphasic scaffolds for repair of deep osteochondral defects in a sheep model, *J. Surg. Res.* 183 (2013) 184–192. doi:10.1016/j.jss.2012.11.036.
- [17] A.M.J. Getgood, S.J. Kew, R. Brooks, H. Aberman, T. Simon, A.K. Lynn, N. Rushton, Evaluation of early-stage osteochondral defect repair using a biphasic scaffold based on a collagen-glycosaminoglycan biopolymer in a caprine model, *Knee.* 19 (2012) 422–430. doi:10.1016/j.knee.2011.03.011.
- [18] C.C. Jiang, H. Chiang, C.J. Liao, Y.J. Lin, T.F. Kuo, C.S. Shieh, Y.Y. Huang, R.S. Tuan, Repair of porcine articular cartilage defect with a biphasic osteochondral composite, *J. Orthop. Res.* 25 (2007) 1277–1290. doi:10.1002/jor.20442.
- [19] E.M. Carlisle, Silicon as an essential trace element in animal nutrition., *Ciba Found. Symp.* 121 (1986) 123–139. doi:10.1002/9780470513323.ch8.
- [20] R. Jugdaohsingh, Silicon and bone health., *J. Nutr. Health Aging.* 11 (2007) 99.
- [21] M.R. Calomme, D.A. Vanden Berghe, Supplementation of calves with stabilized orthosilicic acid: Effect on the Si, Ca, Mg, and P concentrations in serum and the collagen concentration in skin and cartilage, *Biol. Trace Elem. Res.* 56 (1997) 153–165. doi:10.1007/BF02785389.

- [22] M. Hott, C. de Pollak, D. Modrowski, P.J. Marie, Short-term effects of organic silicon on trabecular bone in mature ovariectomized rats, *Calcif. Tissue Int.* 53 (1993) 174–179. doi:10.1007/BF01321834.
- [23] F.H. Nielsen, R. Poellot, Dietary silicon affects bone turnover differently in ovariectomized and sham-operated growing rats, *J. Trace Elem. Exp. Med.* 17 (2004) 137–149. doi:10.1002/jtra.20004.
- [24] P. Valerio, M.M. Pereira, A.M. Goes, M.F. Leite, The effect of ionic products from bioactive glass dissolution on osteoblast proliferation and collagen production, *Biomaterials.* 25 (2004) 2941–2948. doi:10.1016/j.biomaterials.2003.09.086.
- [25] R. Jugdaohsingh, K.L. Tucker, N. Qiao, L.A. Cupples, D.P. Kiel, J.J. Powell, Dietary Silicon Intake Is Positively Associated with Bone Mineral Density in Men and Premenopausal Women of the Framingham Offspring Cohort, *J. Bone Miner. Res.* 19 (2004) 297–307. doi:10.1359/JBMR.0301225.
- [26] E.M. Carlisle, Silicon: A requirement in bone formation independent of vitamin D1, *Calcif. Tissue Int.* 33 (1981) 27. doi:10.1007/BF02409409.
- [27] A.M.H. Ng, K.K. Tan, M.Y. Phang, O. Aziyati, G.H. Tan, M.R. Isa, B.S. Aminuddin, M. Naseem, O. Fauziah, B.H.I. Ruzzymah, Differential osteogenic activity of osteoprogenitor cells on HA and TCP/HA scaffold of tissue engineered bone, *J. Biomed. Mater. Res. - Part A.* 85A (2008) 301–312. doi:10.1002/jbm.a.31324.
- [28] D. Algul, H. Sipahi, A. Aydin, F. Kelleci, S. Ozdatli, F.G. Yener, Biocompatibility of biomimetic multilayered alginate-chitosan/ β -TCP scaffold for osteochondral tissue, *Int. J. Biol. Macromol.* 79 (2015) 363–369. doi:10.1016/j.ijbiomac.2015.05.005.
- [29] Y. Zhou, C. Wu, Y. Xiao, The stimulation of proliferation and differentiation of periodontal ligament cells by the ionic products from Ca₇Si₂P₂O₁₆ bioceramics, *Acta Biomater.* 8 (2012) 2307–2316. doi:10.1016/j.actbio.2012.03.012.
- [30] P. Mainil-Varlet, T. Aigner, M. Brittberg, P. Bullough, A. Hollander, E. Hunziker, R. Kandel, S. Nehrer, K. Pritzker, S. Roberts, E. Stauffer, Histological assessment of cartilage repair: A report by the Histology Endpoint Committee of the International Cartilage Repair Society (ICRS), in: *J. Bone Jt. Surg. - Ser. A*, 2003: pp. 45–57. doi:10.2106/00004623-200300002-00007.
- [31] M. Gosset, F. Berenbaum, S. Thirion, C. Jacques, Primary culture and phenotyping of

- murine chondrocytes, *Nat. Protoc.* 3 (2008) 1253–1260. doi:10.1038/nprot.2008.95.
- [32] S. Picelli, Å.K. Björklund, O.R. Faridani, S. Sagasser, G. Winberg, R. Sandberg, Smart-seq2 for sensitive full-length transcriptome profiling in single cells, *Nat. Methods.* 10 (2013) 1096–1098. doi:10.1038/nmeth.2639.
- [33] S. Anders, P.T. Pyl, W. Huber, HTSeq-A Python framework to work with high-throughput sequencing data, *Bioinformatics.* 31 (2015) 166–169. doi:10.1093/bioinformatics/btu638.
- [34] R. Kolde, pheatmap: Pretty Heatmaps, R Packag. Version 1.0.10. (2018). <https://cran.r-project.org/package=pheatmap>.
- [35] A.W. Robert, A.B.B. Angulski, L. Spangenberg, P. Shigunov, I.T. Pereira, P.S.L. Bettes, H. Naya, A. Correa, B. Dallagiovanna, M.A. Stimamiglio, Gene expression analysis of human adipose tissue-derived stem cells during the initial steps of in vitro osteogenesis, *Sci. Rep.* 8 (2018) 1–11. doi:10.1038/s41598-018-22991-6.
- [36] J. van de Peppel, T. Strini, J. Tilburg, H. Westerhoff, A.J. van Wijnen, J.P. van Leeuwen, Identification of Three Early Phases of Cell-Fate Determination during Osteogenic and Adipogenic Differentiation by Transcription Factor Dynamics, *Stem Cell Reports.* 8 (2017) 947. doi:10.1016/j.stemcr.2017.02.018.
- [37] E. Monaco, M. Bionaz, S. Rodriguez-Zas, W.L. Hurley, M.B. Wheeler, Transcriptomics comparison between porcine adipose and bone marrow mesenchymal stem cells during in vitro osteogenic and adipogenic differentiation, *PLoS One.* 7 (2012) e32481. doi:10.1371/journal.pone.0032481.
- [38] H.M. Van Beuningen, P.M. Van Der Kraan, O.J. Arntz, W.B. Van Den Berg, Protection from interleukin 1 induced destruction of articular cartilage by transforming growth factor β : Studies in anatomically intact cartilage in vitro and in vivo, *Ann. Rheum. Dis.* 52 (1993) 185–191. doi:10.1136/ard.52.3.185.
- [39] X. Yang, L. Chen, X. Xu, C. Li, C. Huang, C.X. Deng, TGF- β /Smad3 signals repress chondrocyte hypertrophic differentiation and are required for maintaining articular cartilage, *J. Cell Biol.* 153 (2001) 35–46. doi:10.1083/jcb.153.1.35.
- [40] G. Li, J. Yin, J. Gao, T.S. Cheng, N.J. Pavlos, C. Zhang, M.H. Zheng, Subchondral bone in osteoarthritis: Insight into risk factors and microstructural changes, *Arthritis Res. Ther.* (2013) 223. doi:10.1186/ar4405.

- [41] M.B. Goldring, S.R. Goldring, Articular cartilage and subchondral bone in the pathogenesis of osteoarthritis, in: *Ann. N. Y. Acad. Sci.*, 2010: pp. 230–237. doi:10.1111/j.1749-6632.2009.05240.x.
- [42] X. Guo, C. Wang, Y. Zhang, R. Xia, M. Hu, C. Duan, Q. Zhao, L. Dong, J. Lu, Y. Qing Song, Repair of large articular cartilage defects with implants of autologous mesenchymal stem cells seeded into beta-tricalcium phosphate in a sheep model., *Tissue Eng.* 10 (2004) 1818–1829. doi:10.1089/ten.2004.10.1818.
- [43] N.F. Soleimani M, Khorsandi L, Atashi A, Chondrogenic differentiation of human umbilical cord blood-derived unrestricted somatic stem cells on a 3D beta-tricalcium phosphate-alginate-gelatin scaffold., *Cell J.* 16 (2014) 43–52.
- [44] C. Deng, H. Zhu, J. Li, C. Feng, Q. Yao, L. Wang, J. Chang, C. Wu, Bioactive scaffolds for regeneration of cartilage and subchondral bone interface, *Theranostics.* 8 (2018) 1940–1955. doi:10.7150/thno.23674.
- [45] W. Wang, D. Rigueur, K.M. Lyons, TGF β signaling in cartilage development and maintenance, *Birth Defects Res. Part C - Embryo Today Rev.* 102 (2014) 37–51. doi:10.1002/bdrc.21058.
- [46] A. Tekari, R. Luginbuehl, W. Hofstetter, R.J. Egli, Transforming growth factor beta signaling is essential for the autonomous formation of cartilage-like tissue by expanded chondrocytes, *PLoS One.* 10 (2015) e0120857. doi:10.1371/journal.pone.0120857.
- [47] E. Mariani, L. Pulsatelli, A. Facchini, Signaling pathways in cartilage repair, *Int. J. Mol. Sci.* 15 (2014) 8667–8698. doi:10.3390/ijms15058667.
- [48] G. Zhen, C. Wen, X. Jia, Y. Li, J.L. Crane, S.C. Mears, F.B. Askin, F.J. Frassica, W. Chang, J. Yao, J.A. Carrino, A. Cosgarea, D. Artemov, Q. Chen, Z. Zhao, X. Zhou, L. Riley, P. Sponseller, M. Wan, W.W. Lu, X. Cao, Inhibition of TGF- β signaling in mesenchymal stem cells of subchondral bone attenuates osteoarthritis, *Nat. Med.* 19 (2013) 704–712. doi:10.1038/nm.3143.
- [49] P.M. Van der Kraan, W.B. Van den Berg, Chondrocyte hypertrophy and osteoarthritis: Role in initiation and progression of cartilage degeneration?, *Osteoarthr. Cartil.* (2012) 223–232. doi:10.1016/j.joca.2011.12.003.
- [50] T.S. Tran, A.L. Kolodkin, R. Bharadwaj, Semaphorin Regulation of Cellular Morphology, *Annu. Rev. Cell Dev. Biol.* 23 (2007) 263. doi:10.1146/annurev.cellbio.22.010605.093554.

- [51] L. Liu, J. Wang, X. Song, Q. Zhu, S. Shen, W. Zhang, Semaphorin 3A promotes osteogenic differentiation in human alveolar bone marrow mesenchymal stem cells, *Exp. Ther. Med.* 15 (2018) 3489–3494. doi:10.3892/etm.2018.5813.
- [52] X. Liu, N. Tan, Y. Zhou, X. Zhou, H. Chen, H. Wei, J. Chen, X. Xu, S. Zhang, G. Yang, Y. Song, Semaphorin 3A Shifts Adipose Mesenchymal Stem Cells towards Osteogenic Phenotype and Promotes Bone Regeneration In Vivo, *Stem Cells Int.* (2016). doi:10.1155/2016/2545214.
- [53] D.R. Rux, D.M. Wellik, Hox genes in the adult skeleton: Novel functions beyond embryonic development, *Dev. Dyn.* (2016) 310–317. doi:10.1002/dvdy.24482.
- [54] D.R. Rux, J.Y. Song, I.T. Swinehart, K.M. Pineault, A.J. Schlientz, K.G. Trulik, S.A. Goldstein, K.M. Kozloff, D. Lucas, D.M. Wellik, Regionally Restricted Hox Function in Adult Bone Marrow Multipotent Mesenchymal Stem/Stromal Cells, *Dev. Cell.* 39 (2016) 653–666. doi:10.1016/j.devcel.2016.11.008.
- [55] P. Leucht, J.-B. Kim, R. Amasha, A.W. James, S. Girod, J.A. Helms, Embryonic origin and Hox status determine progenitor cell fate during adult bone regeneration, *Development.* 135 (2008) 2845–2854. doi:10.1242/dev.023788.
- [56] T.P. Rao, M. Kühl, An updated overview on wnt signaling pathways: A prelude for more, *Circ. Res.* (2010) 1798–1806. doi:10.1161/CIRCRESAHA.110.219840.
- [57] J.H. Kim, X. Liu, J. Wang, X. Chen, H. Zhang, S.H. Kim, J. Cui, R. Li, W. Zhang, Y. Kong, J. Zhang, W. Shui, J. Lamplot, M.R. Rogers, C. Zhao, N. Wang, P. Rajan, J. Tomal, J. Statz, N. Wu, H.H. Luu, R.C. Haydon, T.-C. He, Wnt signaling in bone formation and its therapeutic potential for bone diseases, *Ther. Adv. Musculoskelet. Dis.* 5 (2013) 13–31. doi:10.1177/1759720X12466608.
- [58] M. Okamoto, N. Udagawa, S. Uehara, K. Maeda, T. Yamashita, Y. Nakamichi, H. Kato, N. Saito, Y. Minami, N. Takahashi, Y. Kobayashi, Noncanonical Wnt5a enhances Wnt/ β -catenin signaling during osteoblastogenesis, *Sci. Rep.* 4 (2014) 1–8. doi:10.1038/srep04493.
- [59] A.W. James, Review of Signaling Pathways Governing MSC Osteogenic and Adipogenic Differentiation, *Scientifica (Cairo).* 1 (2013) 684736. doi:10.1155/2013/684736.
- [60] D. Liu, C. Yi, C.-C. Fong, Q. Jin, Z. Wang, W.-K. Yu, D. Sun, J. Zhao, M. Yang, Activation of multiple signaling pathways during the differentiation of mesenchymal stem

cells cultured in a silicon nanowire microenvironment, *Nanomedicine Nanotechnology, Biol. Med.* 10 (2014) 1153–1163. doi:10.1016/j.nano.2014.02.003.

- [61] P. M.F., M. S.C., N.-V.D.L. W.H., V.H. R.J., The biochemical interaction between subchondral bone and cartilage in osteoarthritis, *Osteoarthr. Cartil.* 22 (2014) S352–S353. <http://ovidsp.ovid.com/ovidweb.cgi?T=JS&PAGE=reference&D=emed12&NEWS=N&N=71464383>.